

X-ray detection of PSR 131259-63 at **Periastron**

V. M. Kaspi¹

JPLAC/Caltech/Jet Propulsion Laboratory
Pasadena, CA 91125

M. Tavani²

Columbia Astrophysics Laboratory
New York, NY 10027

F. Nagase³, M. Hirayama⁴, M. Hoshino⁵, T. Aoki⁶
Institute of Space and Astronautical Science
Sagamihara, Kanagawa 229, Japan

N. Kawai⁷

Institute of Physical and Chemical Research
Wako, Saitama, 351-01, Japan

J. Arons⁸

Department of Astronomy and Department of Physics, University of California
Berkeley, CA 94720

ABSTRACT

We report on results of X-ray observations of the unique radio pulsar/white star binary PSR 1312.59-63 / SS2883, obtained using the *ASCA* satellite two weeks before, during, and two weeks after the pulsar's most recent periastron passage on January 9, 1994. The source was detected at all three epochs, with an X-ray

¹Hubble Fellow; Visiting Associate, Caltech Astronomy Department; E-mail: vicky@ipac.caltech.edu

²E-mail: tavani@carmen.phys.columbia.edu

³E-mail: nagase@astro.isas.ac.jp

⁴E-mail: hirayama@tkynext2.astro.isas.ac.jp

⁵E-mail: hoshino@gtl.isas.ac.jp

⁶E-mail: aoki@astro.isas.ac.jp

⁷E-mail: nkawai@postman.riken.go.jp

⁸E-mail: arons@astroplasma.berkeley.edu

luminosity in the 1-10 keV band of $\sim 1 \times 10^{34} (d/2 \text{ kpc})^2 \text{ erg s}^{-1}$ at the pre- and post-periastron epochs, and a factor of ~ 2 smaller at periastron. The X-ray emission can be characterized by power-law spectra with a photon index in the range 1.5- 1.9, with evidence for spectral softening at periastron. The photoelectric absorption, $N_H \sim 5 \times 10^{21} \text{ cm}^{-2}$, was constant for the three observations within measurement uncertainties, and is consistent with the galactic contribution. We detect no pulsations, and derive an upper limit on periodicities close to the PSR B1259-63 spin period of $\sim 7\%$ of the total observed flux, conservatively assuming a sine-wave profile. We argue that accretion of gaseous material onto the surface of the neutron star is an unlikely origin for the observed X-rays. The characteristics of the X-ray emission from the PSR B1259-63 system are in good agreement with models of non-thermal acceleration of relativistic particles from the pulsar wind in a shock at the location where the pulsar and Be star wind pressures balance. Assuming reasonable Be star equatorial outflow and pulsar wind parameters, we find that the mass loss rate \dot{M} and surface velocity v are constrained by the relation $10 \lesssim (v/10 \text{ km s}^{-1})(\dot{M}/10^{-8} M_\odot \text{ yr}^{-1}) \lesssim 100$.

Subject headings: pulsars: individual: PSR B1259-63 stars: neutron - stars: individual: SS2883 - binaries: eclipsing - stars: emission line, Be - x-rays: stars

1 INTRODUCTION

PSR 111259-63 is a 47 ms radio pulsar discovered by Johnston *et al.* (1992b) in a survey of the southern galactic plane for radio pulsars (Johnston *et al.* 1992a). The pulsar's astrometric and spin parameters, as determined by radio timing observations (Johnston *et al.* 1994) are given in Table 1. The short pulse period suggests that the pulsar is either young like the Crab pulsar, or a member of the "recycled" class of pulsars in which the short period is the result of a past episode of mass and angular momentum accretion. However, the pulsar's short characteristic age and high surface magnetic field (see Table 1), as well as the absence of any known supernova remnant in the vicinity, imply that neither is likely to be the case.

The radio timing observations have shown that the pulsar is in a 3.4 yr, highly eccentric binary orbit. The observed Keplerian orbital parameters are provided in Table 1. The pulsar's mass function implies its orbital companion has a mass greater than $3.2 M_\odot$ assuming a $1.4 M_\odot$ neutron star. Optical observations in the direction of the pulsar reveal a 10th mag

B2e star, SS 2883, at a position coincident with the pulsar's timing position. Johnston *et al.* (1992b) conclude SS 2883 is the pulsar's companion, and from the spectral type! Johnston *et al.* (1994) deduce a mass for SS 2883 of $\sim 10M_{\odot}$ and a radius of $\sim 6R_{\odot}$. A radio eclipse was observed by Johnston *et al.* (1992b) during the last periastron passage in 1990, however detailed monitoring was not carried out because only at that epoch was the duplicity recognized.

Among over 600 known radio pulsars, the PSR B1529-63 system is the only Be star/pulsar binary. A similar binary system, PSR J0045-7319 in the Small Magellanic Cloud, consists of a 0.926 s pulsar in orbit with a B star. However optical observations show neither evidence for emission lines, nor any eclipse of the radio signal near periastron (Bell *et al.* 1995; Kaspi *et al.* 1994).

The distance to the PSR B1529-63 system is uncertain. From the dispersion measure (DM) of the pulsar and a model for the galactic electron distribution (Taylor & Cordes 1993), the estimated distance is $d = 4.6$ kpc. However, DM-derived distances are often uncertain within a factor of ~ 2 . Johnston *et al.* (1994) argue on the basis of photometric observations that the distance to SS 2883 cannot be greater than 1.5 kpc, in conflict with that deduced from the pulsar DM.

Be stars are characterized by strong optical emission lines of ionized hydrogen, and excess continuum radiation, likely due to free-free emission, at infrared and radio wavelengths, all of which suggest the presence of a dense, slowly expanding wind (e.g. Slettebak (1988) and references therein). However, UV observations of asymmetric blueshifted absorption in resonance lines of C IV and Si IV suggest the presence of a fast, low-density wind (Snow 1982). These seemingly contradictory observations are reconciled in the so-called "disk" model (e.g. Waters 1986), in which the $H\alpha$ emission and infrared excesses are produced in a dense, slowly-expanding equatorially concentrated wind, with a fast, tenuous wind in the polar region. The disk model is largely empirical, however the equatorial concentration is likely a result of relatively large stellar angular velocities (e.g. Bjorkman & Cassinelli 1993). Typical mass-loss rates in the disk regions of Be stars are in the range $10^{-9} M_{\odot} \text{ yr}^{-1} \lesssim \dot{M} \lesssim 10^{-6} M_{\odot} \text{ yr}^{-1}$ (e.g. Waters *et al.* 1988 and references therein.) No direct estimate of the mass-loss rate of SS 2883 has been published.

Radio pulsars lose their rotational energy by a relativistic magnetized wind composed of electrons, positrons and possibly heavy ions, which occasionally is seen to energize surrounding gaseous nebular material, resulting in the emission of high-energy radiation. The best example of currently known pulsar-driven nebular emission is the Crab nebula, in which the efficiency of conversion of spin-down energy into unpulsed X-ray emission is observed to be $\sim 10\%$; such highly efficient X-ray emission is believed to be the result of MHD shock

acceleration of relativistic pulsar wind particles at the location where the pulsar wind and ambient medium pressures balance (Rees & Gunn 1974; Kundt & Krotscheck 1980; Kennel & Coroniti 1984; Hoshino *et al.* 1992). Pulsar bow shock nebulae, in which a high-velocity pulsar's wind is seen interacting with the surrounding interstellar medium, also provide information on pulsar winds (e.g. Kulkarni & Hester 1988; Bell, Bailes & Bessell 1993; Cordes, Romani & Lundgren 1993). However, these systems are expected to be weak high-energy emitters (Arons & Tavani 1993).

In contrast to the nebular environments of previously known interacting pulsars, the nature of the PSR 111259-63 system naturally allows the study of time-dependent pulsar/nebula interactions, because the radio pulsar unavoidably interacts with the Be star outflow each periastron passage (Kochanek 1994; Tavani 1994). The pulsar radiation pressure might be large enough to withstand the compressing ram pressure force due to the gaseous outflow from the 1 Be star, even at periastron. If so, an interesting time-variable interaction of the pulsar wind with the mass outflow is expected (Tavani, Arons & Kaspi 1994, hereafter TAK94). Alternatively, for a large Be star mass outflow, accretion might occur, and bright X-ray emission could result. The 69 Ins X-ray pulsar A0538-66 is in an eccentric orbit around a 1 Be star and occasionally accretes with an X-ray luminosity near the Eddington limit, demonstrating the ability of mass outflows from massive companions to cause accretion onto rapidly rotating neutron stars (Skinner *et al.* 1982).

About 20 Be/neutron star X-ray emitting binaries are known in the Galaxy. These have orbital characteristics similar to PSR B1259-63: long orbital periods and high eccentricities (van den Heuvel & Rappaport 1987). The Be/X-ray binaries form a subclass of the high-mass X-ray binaries, which show pulsed X-ray emission with periods in the range $0.069 \text{ s} \lesssim P \lesssim 10^3 \text{ s}$, the signature of accretion onto the surface of a strongly magnetized neutron star (Nagase 1989). Radio pulsations have never been detected from any high-mass X-ray binary system. The PSR 111259-63 system is therefore unique among Be/neutron star binaries in that the neutron star is also a radio pulsar.

X-ray emission was detected the PSR 111259-63 system near apastron. The first low-level X-ray detection was by Cominsky, Roberts & Johnston (1994) (hereafter CRJ94) who observed the system just after apastron using *ROSAT* in September 1992. The observed X-ray luminosity in the *ROSAT* band was $0.38 \times 10^{33} \text{ erg s}^{-1}$, for $d = 2 \text{ kpc}$ and depending on the assumed spectral model. A recent analysis of public archive *ROSAT* data taken in February 1992, just before apastron, reveals significant X-ray emission at a level approximately consistent with the CRJ94 result (Greiner, Tavani & Belloni 1994, hereafter GTB95). Statistics in both detections are poor and little spectral information is available. The observed X-ray luminosities near apastron, though dependent on the assumed spectrum, are

larger than expected from coronal emission from a typical 1 Be star. Since the radio pulsations were detected at the epochs of all *ROSAT* observations, accretion of material onto the neutron star is an unlikely explanation, since it would have quenched the radio emission.

In this paper, we report on three X-ray observations with the *ASCA* satellite at the system's most recent periastron passage. The X-ray observations were part of a multiwavelength campaign to study the emission near periastron, including UV and optical (McCullum, Castelaz & Bruhweiler 1995), hard X-ray and gamma ray (Grove *et al.* 1995), and radio observations (Johnston *et al.* 1995). Preliminary reports indicate that the pulsed radio emission became undetectable in mid December 1993 and became visible again only at the beginning of February 1994 (S. Johnston and R.N. Manchester, personal communication). Thus, the *ASCA* observations reported here were all obtained during the radio eclipse.

2 OBSERVATIONS

In order to monitor possible time variability of the X-ray emission, the *ASCA X-ray* satellite observed the system near periastron, and approximately two weeks before and after periastron. The first and third observations had exposure times of $\sim 20,000$ s, while the second had $\sim 40,000$ s. Table 2 gives a summary of the three *ASCA* observations and of the orbital geometry for an assumed Be star mass $M_c = 10 M_\odot$. In Figure 1 we provide a schematic drawing of the pulsar's orbit around the systemic center of mass, together with the approximate location of the pulsar during the X-ray observations reported by CRJ94, GT1395, and those described here.

The *ASCA* satellite (formerly Astro-D) carries four X-ray telescopes (XRTs), each consisting of nested concentric thin foils that approximate paired hyperbolic and parabolic surfaces. The X-ray telescopes have pass band 0.5–12 keV and spatial resolution $\sim 1'$. At the focus of two of the telescopes are Solid-state Imaging Spectrometers (SIS), each of which is based around four CCD chips having energy resolution 2% at 5.9 keV and field of view $11' \times 11'$. At the focus of the other two telescopes are Gas Imaging Spectrometers (GIS), imaging gas scintillation proportional counters with 8% energy resolution at 5.9 keV and a circular field of view with diameter $50'$. All three of our observations were done using both SIS and GIS instruments. The instruments are described in more detail by Tanaka, Inoue & Holt (1994).

The data reduction was done at the *ASCA* Guest *observer* Facility (GOF) at the Goddard Space Flight Center and at the Institute for Space and Astronautical Science in Japan. The program XSELECT from the FTOOLS software package was used to identify the

pulsar and select a circular region centered on the source from the fields of view of each instrument. For GIS observations, the circular region had radius $6'$, while for the SIS data the region had radius $4'$. Background subtraction was done using GOF-supplied background files. Hot and flickering pixels were removed from the SIS data. Binned photon lists were created for spectral analyses (rebinning to 64 spectral bins for GIS and 256 for SIS was done after extraction), as were time-tagged photon event files for the timing analyses, with barycentric corrections done using the GOF-supplied routine BARYCFN. The pulsar's barycentric pulse period as a function of time is shown in the top panel of Figure 2. The high-lighted regions show the epochs and durations of our *ASCA* observations; both the change in observed barycentric period from epoch to epoch as well as the small period variation within each observation is apparent. This is discussed further in §3.2.

Response matrices were produced using GOF-supplied detector response functions and XRF effective area curves using the *ASCA*ARF software. The GIS data had time resolution 0.976 or 0.488 ms, depending on the telemetry mode, and were used for the timing analysis described below. The SIS data have poor temporal resolution but excellent spectral resolution, so were used only for the spectral analysis.

3 RESULTS

At all three observing epochs, a point source was detected at a position consistent with that of the pulsar, given the $\sim 1'$ uncertainty of the *ASCA* pointing. An image from the GIS detector for the second observation is shown in Figure 3; images of the field for the first and third observations are similar. The brighter source seen in the image is the pulsar. The SIS image of the field (Figure 4) shows the typical *ASCA* "cross-pattern" at the position of the pulsar, consistent with its identification as a point-source; SIS images for all three observations are similar. Count rates for the four instruments are given in Table 3. Figure 5 shows the light curves for GIS2 data at all three observing epochs; those for the other instruments are similar. We note the absence of any rapid variability in the X-ray flux.

The second source seen in the GIS field of view approximately $10'$ south west of the pulsar system is a previously unidentified X-ray source, serendipitously discovered as part of this effort. The serendipitous source does not appear in the SIS images since it lies outside the smaller SIS field of view. We do not consider the serendipitous source further in this paper, apart for some brief remarks in §3.3. A more careful analysis of this new X-ray source is planned.

3.1 Spectral Results

The spectral analysis was done with the NASA/GSFC XSPEC software package. SIS spectra for the three observations are shown in Figure 6. We found that a simple power law describes the data well at all three epochs. No evidence was found for any line features in the spectra. The results of three-parameter fits to the 256-spectral bin SIS data (SIS0 and SIS1 combined) are given in Table 4. The χ^2 fit statistic is only slightly higher for a thermal bremsstrahlung model compared with that for the power-law model; thus, from the *ASCA* data alone, a thermal model, with $kT \sim 10$ keV, $N_H \sim 0.4 \times 10^{22}$ cm $^{-2}$, and fluxes equal to those found with the power law model cannot be excluded. However, hard X-ray emission in the energy range 50-200 keV from the direction of the PSR 111259-63 system was detected by the *OSSLE* instrument aboard the *Compton Gamma-Ray Observatory* during an observation from January 3-23, 1994, and had a spectrum consistent with a simple extrapolation of the power law fit to the *ASCA* data reported here, thus ruling out a thermal model (Grove *et al.* 1995). The GIS data are in agreement with the SIS data to within $\sim 30\%$, consistent with known systematic differences due to calibration uncertainties. The uncertainties quoted in the Table for the SIS data are statistical 90% confidence intervals as calculated by XSPEC, and do not include any estimate of systematic calibration uncertainties. In Figure 7 we show contour plots of the N_H and photon index parameter uncertainties, holding the 1-10 keV flux fixed at the values in Table 4. The contours plotted are 68%, 90% and 99% confidence levels.

An important result of these observations concerns the determination of the column density N_H . We find that the photoelectric absorption toward the source, $N_H = (0.53 \pm 0.05) \times 10^{22}$ cm $^{-2}$, is consistent with an intrinsically unabsorbed source in the galactic plane at the estimated distance of PSR B1259-63. We find no evidence for any significant variation in the absorption with orbital phase within the measurement uncertainties. Our measurement of N_H is consistent with the approximate values obtained independently near apastron from the *ROSAT* observations (CRJ94, GT1395). We discuss the absorption further in §4.

As is clear from Table 4, the X-ray flux from the source was time-variable, having reached a minimum at periastron that corresponds to about half the values symmetrically around periastron.

3.2 Search for Pulsations

X-ray emission modulated with the PSR B1259-63 spin period can be produced by several mechanisms: (1) magnetospheric pulsed emission (e.g. Seward & Harnden 1982) (2) reprocessing at the neutron star polar cap of energy from the precipitation of electron/positron pair currents (e.g. Harding 1995) (3) accretion of gaseous material channeled by the strong surface magnetic field into an X-ray radiating accretion column, as in the case of the rapidly rotating X-ray pulsar A0538-66 during its outbursts (Skinner *et al.* 1982).

To determine whether any of these mechanisms has produced the observed X-ray emission, we searched for pulsations in the PSR B1259-63 data, using the ephemeris provided by the radio data shown in Table 1 (Johnston *et al.* 1994). For the timing analysis, only GIS data were used because of their high time resolution. Table 5 summarizes the characteristics of the *ASCA* data that are relevant to the pulsation search.

As shown in Figure 2, the pulse period of PSR B1259-63 changed significantly during each of our observations because of the varying Doppler shift due to the large acceleration of the pulsar in its eccentric orbit near periastron. In general, a variable Doppler shift on a pulsed signal can be neglected if the distance the source has traveled during the integration time T due to acceleration a , $d = aT^2/2$, is much less than the distance between emitted wavefronts $L = cP$. For the three *ASCA* observations of the PSR B1259-63 system, the condition $d \ll L$ is not verified. However, the variation in the observed period because of the acceleration of the pulsar in its orbit is well-approximated by a linear trend for our observations. Thus, to search for pulsations, we folded the photons modulo trial periods near the expected pulse period, after having corrected the arrival times for the acceleration of the pulsar in two different ways: using the orbital parameters given by Johnston *et al.* (1994) (§3.2.1) and by correcting for a number of trial linear trends in the period (§3.2.2).

3. 2.1 Epoch-folding with Orbital Doppler Shift Correction

Prior to searching for pulsations, the orbital Doppler shift of the pulse period, given by

$$\delta P(t) = \frac{2\pi P a_p \sin i}{P_b(1-e^2)^{1/2}} [\cos(\omega + \phi(t)) - e \cos \omega] \quad (1)$$

to first order (e.g. Shapiro & Teukolsky 1983), where $\phi(t)$ is the true anomaly, was accounted for using standard methods. Epoch-folding of the corrected photon arrival times was done using the X-ray timing software package XRONOS (Stella & Angelini 1992). For each *ASCA* observation, photon arrival times corrected for the orbital motion were folded with $n = 32$ time bins across the pulse profile at periods in the interval $P \pm \Delta P$, with $P = 47.7623$ ms. A total of 128 trial periods were searched, with period steps of half the Fourier

step, $\delta P = P^2/2T$. The corresponding period range ΔP was 1.5×10^{-6} s for the first and third *ASCA* observations, and 6×10^{-7} s for the second observation.

For each trial period, an estimate of the likelihood of the existence of a pulse in the folded data was computed using the quantity

$$S = \sum_{k=1}^n \frac{(C_k - C)^2}{\sigma_k^2}, \quad (2)$$

where C_k is the observed count rate of the k th phase bin, C is the average count rate, and $\sigma_k^2 = 21(7/P)$ (Leahy *et al.* (11, 1983)). For our observations σ_k^2 is constant. A coherent pulsation in the data results in a value for S large compared with noise. In the limit of a large number of photons $N_\gamma = CT$, S is the familiar χ_{n-1}^2 . A plot of the statistic S versus trial period for one of the observations is shown in Figure 8. No statistically significant peak in the S distributions for any of the three observations was detected. We estimated an upper limit to the pulsed fraction using the analytical methods described by Leahy *et al.* (1983). In this way, we compute 90% confidence upper limits on the pulsed fractions, conservatively assuming a sine-wave profile. These are given in Table 5.

Similar epoch folding analyses were done on short stretches of data in which the variable Doppler shift was negligible. In addition, similar analyses were done on the GIS2 and GIS3 data sets separately, in case an unknown clock discrepancy exists between the two instruments. In no instance was there any evidence for pulsations in the data. In addition, a similar analysis was done using epoch folding and the Z_n^2 test (Buccheri *et al.* 1983) for $n=2, 3$; no evidence for pulsations was found.

3.2.2 Epoch-folding by Searching in $P - \dot{P}$ Space

Since the variation in the pulse period due to a variable Doppler shift over the course of each observation is well-modeled by a linear trend, as an additional check, we searched for pulsations in $P - \dot{P}$ space. This “acceleration search” is motivated by the possibility of small biasing of the orbital parameters obtained by Johnston *et al.* (1994) using radio timing, due perhaps to unmodeled dispersion delays, unmodeled post-Keplerian dynamical effects (Lai, Bildsten & Kaspi 1995), or simply because their determination was based on fewer than two complete orbits. The maximum accretion torque on the pulsar, assuming Eddington rate accretion at the corotation radius, gives $\dot{P} \approx 3 \times 10^{-11} (P/1 \text{ s})^{7/3}$, which, for our observations of PSR B1259-63, is negligibly small. Since XRONOS cannot do acceleration searches, it was not used for this part of the analysis.

With no variable Doppler shift correction done to the photon arrival times, they were folded at a range of trial P 's and \dot{P} 's using $n = 8, 16,$ and 32 bins across the pulse period, to ensure sensitivity to a variety of pulse duty cycles. Steps in P were done oversampling the Fourier step by a factor of 5, that is $\delta P = P^2/5T$. The optimal step in \dot{P} was chosen to be that which results in the worst case photon arrival time 180° out of phase with the pulse, $\delta \dot{P} = (P/T)^2$, and was also oversampled by a factor of 5. The statistic S was computed for each folded profile using Equation 2. Plots of S versus P and \dot{P} were examined for significant features; none was found. To estimate an upper limit to the pulsed fraction, fake pulsed photon arrival times were injected into the data. The fraction of fake arrival times was adjusted until it produced a feature in the S plots consistent with features seen in the real data. Using this method, we conclude that for pulse profiles having widths less than $1/8$ of the pulse period, less than 2% of the flux was pulsed at each epoch.

3.3 Serendipitous Source

Figure 3 shows a second source in the GIS field of view, $\sim 10'$ southwest of the pulsar, outside the SIS field of view in all our observations. Although the source appears slightly elongated in the image shown in Figure 3, given its location far off-axis, its apparent morphology is roughly consistent with a point source. The source was present in all three of our observations, and showed no strong variability on short time scales. However, there was some evidence for a small monotonic increase in its count rate from the first to the third observation. A power law spectral model provides a reasonable fit to the data, although given the limited statistics, other models cannot be ruled out with any certainty. Assuming a power law, the absorption toward the source, $N_H \sim 3 \times 10^{22} \text{ cm}^{-2}$, suggests it is considerably more distant than PSR B1259--63. A search through the Simbad database reveals no catalogued sources within $\sim 5'$ of this source.

4 DISCUSSION

We consider here various possible origins of the X-ray emission from the PSR B1259--63 system near periastron.

4.1 X-ray emission from the Be Star

As discussed by CRJ94, early-type B stars have been shown to emit X-rays that are explained as originating from a radiation-driven wind heated by shocks (Lucy 1982; MacFar-

lane & Cassinelli 1989; Bjorkman & Cassinelli 1993), with X-ray luminosities, L_x , observed to scale roughly with the bolometric luminosities, L_{bol} , with proportionality constant $\sim 10^{-7}$ (Pallavicini *et al.* 1981). In a recent *ROSAT* survey of OB and OBe stars, Meurs *et al.* (1992) found a similar relationship, albeit with considerable scatter, with *ROSAT* L_x/L_{bol} ranging from 10^{-8} to 10^{-4} . Cassinelli *et al.* (1994) used *ROSAT* observations of B and Be stars to show that there is a transition in X-ray properties as a function of spectral type, with L_x/L_{bol} smaller for stars later than B11. Using our observed *ASCA* X-ray fluxes extrapolated to the *ROSAT* band and the L_{bol} for SS 2883 of $5.8 \times 10^4 L_{\odot}$ (Johnston *et al.* 1992)), we find $L_x/L_{\text{bol}} \sim 10^{-3}$, much larger than would be predicted by the empirical relationship. Furthermore, Cassinelli *et al.* (1994) showed that X-ray spectra of main and near-main sequence B stars are characterized by emission from gas at a temperature of $\sim 2 \times 10^6$ K, with the hottest X-ray source in their sample having a temperature 9×10^6 K. By contrast, our thermal spectrum fits to the *ASCA* data for PSR 111259-63 are characterized by much higher temperatures, $T \sim 10^8$ K (see §3.1). In any case, as discussed in §3.1, *OSSR* observations by Grove *et al.* (1995) rule out a thermal spectrum. Thus the Be star is an unlikely source of the observed X-rays.

4.2 X-ray emission from the neutron star surface or magnetosphere

Short-period pulsars are occasionally observed to emit X-rays (see Ögelman 1995 for a review). Although high-energy emission is generally associated with pulsars having much smaller characteristic ages than that of PSR B11259-63, its short pulsation period of 47 ms makes it a plausible X-ray emitter. X-rays from isolated neutron stars are observed in two different forms: X-rays are either produced in the form of pulsations (e.g. Fritz *et al.* 1969; Seward & Harnden 1982; Seward, Harnden & Helfand 1984), or in weak unpulsed thermal emission arising from the cooling of the neutron star (e.g. Córdova *et al.* 1989; Halpern & Ruderman 1993). The unpulsed and non-thermal emission rules out both these possibilities.

4.3 X-ray emission from accretion onto the neutron star surface

The gravitational accretion radius is given by

$$R_G \equiv \frac{2GM_p}{v_{\text{rel}}^2} \simeq \frac{3 \times 10^{12} \text{ cm}}{(v_{\text{rel}}/100 \text{ km s}^{-1})^2} \quad (3)$$

where v_{rel} is the relative wind/orbital velocity. As shown by TAT(94), for reasonable assumptions about the pressures of the pulsar and Be star winds, the radius at which the

two pressures balance is well outside the gravitational accretion radius, at all orbital phases. Thus, they concluded that accretion would be unlikely to occur, even near periastron, unless the Be star possessed an unusually strong wind.

Parametrizing the Be star wind by $\Upsilon \equiv \dot{M}_{-8} v_6$, where the Be star mass-loss rate $\dot{M} \equiv (10^{-8} M_{\odot} \text{ yr}^{-1}) \dot{M}_{-8}$, and the wind velocity at the stellar surface $v \equiv (10^6 \text{ cm s}^{-1}) v_6$, TAK94 showed that accretion was possible near periastron only for $\Upsilon > 100$ for standard pulsar wind parameters and characteristics of the Be star outflow. Under these conditions, accretion onto the neutron star should yield an X-ray luminosity $L_x \simeq GM_p \dot{M} / R_p \simeq 1.2 \times 10^{38} \dot{M}_{-8} \text{ erg s}^{-1}$, assuming $M_p = 1.4 M_{\odot}$ and $R_p = 10 \text{ km}$ for the neutron star mass and radius respectively. Thus, the expected L_x in this scenario is several orders of magnitude greater than the observed value of $\sim 1 \times 10^{34} (d/2 \text{ kpc})^2 \text{ ergs s}^{-1}$.

Other evidence against accretion is provided by the absence of X-ray pulsations at any orbital phase. The surface magnetic field strength of PSR B1259-63 is $B = 3.3 \times 10^{11} \text{ G}$. This field strength should easily be sufficient to channel any infalling matter onto the stellar surface near the poles, which should result in a strongly anisotropic angular pattern of emission (Nagase 1989). The observability of X-ray pulsations from the PSR J1259-63 system depends somewhat on the geometry of inclination of the pulsar magnetic axis with respect to the line of sight, however accretion without pulsations requires finely tuned geometries.

There are several additional arguments against accretion. The observed reddening toward SS 2883, $A_v = 3.25 \text{ mag}$ (Westerlund & Garnier 1989), implies an expected $N_{\text{H}} \sim 7 \times 10^{21} \text{ cm}^{-2}$ (Gorenstein 1975). This is in rough agreement with the observed value of $\sim 5 \times 10^{21} \text{ cm}^{-2}$. Thus, the X-ray absorption is consistent with that from the galactic contribution. The observed absence of temporal variation of N_{H} as PSR B1259-63 moved around the periastron region can be used to rule out the presence of a large quantity of absorbing material intrinsic to the system as expected from accretion models of the PSR B1259-63 system (Tavani & Arons 1995, hereafter TA95). Furthermore, spectra at all three epochs show no features, such as Fe $K\alpha$ emission lines, seen in spectra of known accreting, high-magnetic field systems (Nagase 1989). Also, the *OSSF* results demonstrate the absence of any spectral cutoff, commonly observed in accreting systems (White, Swank & Holt 183). Furthermore, accreting sources commonly show strong, rapid variability (e.g. SMC X-1, K. Ebisawa, personal communication); by contrast, the light curves for PSR B1259-63 are stable (Figure 5).

Finally, a fourth *ASCA* observation of PSR B1259-63 made after the radio pulsations reappeared (Hirayama *et al.* 1995), shows very similar X-ray characteristics to those reported here, rendering an accretion scenario, in which radio pulsations should be quenched, highly unlikely.

The absence of accretion implies the pulsar wind was able to withstand the pressure of the Be star mass outflow, which implies $T \lesssim 100$ assuming a large fraction of the pulsar spin-down energy goes into its wind (TAK94).

4.4 X-ray emission from captured material outside the pulsar light-cylinder

King & Cominsky (1994), hereafter KC94 proposed a model to explain the observed apastron X-rays as being due to the release of gravitational potential energy of gaseous material falling to a boundary radius, defined to be the location at which the pulsar magnetic pressure balances the ram pressure of the infalling gas. In this model, the boundary radius, unlike the canonical magnetospheric radius, is located outside of the light-cylinder. The motivation for such a scenario came from the fact that at apastron, both radio pulsations and X-ray emission were detected.

This model has difficulty accounting for the X-ray observations reported here. First, it does not account for the pulsar wind pressure, observed to be important in numerous other radio pulsar systems (e.g. Kennel & Coroniti 1984; Kuulkarni & Hester 1988; Cordes, Romani & Lundgren 1993; Bell, Bailes & Bessell 1993). The wind pressure, as discussed above, would otherwise keep material from approaching the pulsar. Second, even at apastron, KC94 found a boundary radius very close (within a factor of two) to the light-cylinder⁹; at periastron where the Be star wind density is at least three orders of magnitude larger, it is difficult to see how matter, if it could overcome the pulsar wind pressure, would not penetrate the light cylinder and result in standard accretion, already discussed in §4.3 above. Also, KC94 required the Be star to have an outflow velocity in the apastron region that was much smaller with those determined for other Be stars by independent means (Waters *et al.* 1988); to explain the periastron X-rays, the outflow in the periastron region would have to be much faster than at apastron, which would also be at odds with the results of Waters *et al.* (1988). We conclude this model is an unlikely explanation for the observed X-rays.

4.5 Shock Emission

The difficulties canonical accretion and gravitational capture models have explaining the characteristics of the X-ray emission from the PSR B1259–63 system suggest that an

⁹We note that KC94 used a dipolar magnetic field outside the light-cylinder in their pressure balance calculation. Using the correct $1/r$ field dependence does not change this result much for their input parameters.

alternative mechanism of emission is at work. A natural candidate for the origin of the unpulsed X-rays of moderate luminosity and low photoelectric absorption reported in this paper is magnetohydrodynamic shock-powered radiation. Shock acceleration of the Crab pulsar pairs accounts well for many of the spectral and morphological properties of the high-energy emission from the Crab nebula (Kennel & Coroniti 1984; Gallant & Arons 1994). The relativistic reverse shock formed in the pulsar's wind just interior to the boundary between the decelerated pulsar wind and the Be star wind is the likely site of analogous shock particle acceleration in the PSR 111259-63 system.

As discussed by TAK94, there are two important radiative cooling mechanisms that can be effective in the PSR B1259-63 system. One is synchrotron cooling of the pairs in the pulsar magnetic field, which becomes more efficient as the shock approaches the pulsar. The other is inverse Compton scattering in the background optical photons from the radiating photosphere of the Be star, which becomes more efficient as the shock approaches the Be star. However, if the shock acceleration time is short compared to radiative cooling time scales, the flow in and just behind the shock is nonradiative, and shock acceleration is able to achieve a pair power-law spectrum. Thus, the radiative properties of the relativistic electron/positron pairs in the pulsar wind depend on the extent to which the shock acceleration mechanism is effective, which in turn depends on the location of the shock. In the PSR B1259-63 system, the size of the pulsar cavity, hence the distance of the shock from the surface of the Be star, depends on the wind properties. For a range of wind parameters in the PSR 111259-63 system corresponding to a shock located at intermediate distances, TAK94 showed that the shock acceleration time scale is shorter than the cooling time scales. Hence, in this regime, a non-thermal spectrum is expected, and will extend from X-ray energies to $\sim 1-10$ MeV for an upstream flow Lorentz factor of the pulsar's wind $\gamma \sim 10^6$, similar to that found in models of the response of the Crab Nebula to the wind from its pulsar."

The non-thermal nature of the *ASCA* spectrum, as corroborated by the *OSS1* detection (Grove *et al.* 1995), does not agree with the quasi-thermal spectrum expected for $\Upsilon \gtrsim 10$ for strong inverse Compton cooling for a shock radius close to the surface of the Be star, assuming the fraction of the pulsar spin-down energy that goes into a wind is of order unity. Our results favor a shock radius at an intermediate distance between the Be star and PSR B1259-63, with $\Upsilon \gtrsim 10$, and a shock acceleration time scale less than or comparable with the synchrotron time scale near periastron (case A of the non-thermal "compact" nebular emission of TAK94). The observed efficiency of conversion of spin-down pulsar energy into X-ray emission in the *ASCA* band at periastron is $L_x/\dot{E} \simeq 0.9(d/2 \text{ kpc})\%$, and approximately twice this value at the pre- and post-periastron epochs. The variability of the X-ray emission and spectrum of the PSR 111259-63 system near periastron can be due to an increase of synchrotron cooling near periastron with consequent modification of the

emission properties of the shock, including a change in luminosity in the *ASCA* band as well as a change in the photon index, as is observed. Alternatively, misalignment of the orbital and Be star equatorial planes, or time-variability in the Be star wind may be important.

The shock model outlined here is consistent with all shock acceleration processes which satisfy the constraint that the acceleration time in and just behind the shock is short compared to the synchrotron and inverse Compton radiative loss times. In particular, this constraint is satisfied by the magnetosonic wave absorption theory of Hoshino *et al.* (1992) which applies to the quasi-transverse shock geometry appropriate to the termination shock of this pulsar's wind; it is not satisfied by the diffusive Fermi process in quasi-parallel relativistic shocks, as studied by Ellison, Jones & Reynolds (1990). A detailed study of the constraints on the shock acceleration physics and on the complex interplay among different radiation mechanisms for the PSR B1259-63 system will be presented elsewhere (TAA95).

5 SUMMARY

We have reported on three X-ray observations of the unique radio pulsar/Be star binary system PSR B1259-63 obtained near periastron using the *ASCA* satellite. At all three epochs, the source was observed to have moderate X-ray luminosity $\sim 10^{34}$ erg s⁻¹ in the *ASCA* band, and absorption $N_H \sim 5 \times 10^{21}$ cm⁻², consistent with that expected from the galactic contribution alone. No X-ray pulsations were detected. The observed X-ray spectra are all consistent with simple power laws. Some of the X-ray characteristics varied in the three observations: the X-ray luminosity was a factor of ~ 2 smaller, and there was some evidence for a softening of the spectrum at periastron. The absorption, by contrast, was constant for the three observations.

We conclude that accretion onto the neutron star is an unlikely explanation for the observed X-rays, both those reported here, and those observed near apastron. Any model involving accretion would have to explain the following observations, none of which is typical of other known accreting sources: a radio pulsar wind pressure was overcome with only moderate X-ray luminosity; no pulsations were detected; no absorption intrinsic to the source was seen; no features were observed in spectrum; no spectral cutoff is observed (Grove *et al.* 1995); no strong, rapid variability is observed; and radio pulsations were visible near the same epoch as the X-rays (Hirayama *et al.* 1995). Since accretion is unlikely, the Be star wind could not overcome the pulsar wind pressure, which implies $\Upsilon \lesssim 100$.

By contrast, magnetohydrodynamic shock acceleration of relativistic electron/positron pulsar wind pairs provides a natural way to account for the observations reported here. In the framework outlined by TAAK94, our observations constrain the Be star wind to have $\Upsilon \lesssim 10$.

A detailed interpretation of the results reported here in terms of the shock acceleration mechanism will appear elsewhere (TVA95).

Careful monitoring of high-energy emission from PSR B1259-63 at other orbital phases will be useful for further constraining properties of the pulsar wind and the shock acceleration mechanism. Be stars are well-known to have episodes of enhanced mass loss, and the possibility of accretion of Be star wind material onto the neutron star during a future outburst, especially near periastron, cannot be discounted. Indeed, our observations cannot rule out brief episodes of accretion due to a variable Be star wind in the intervals between the *ASCA* observations, however radio timing data obtained before and after periastron should be useful for setting limits on external torques experienced by the pulsar, which in turn set a limit on the amount of material accreted.

6 Acknowledgements

We are indebted to the staff of the *ASCA* Guest Observers Facility, especially to K. Ebisawa, J. Gotthelf, N. White and L. Angelini. This work was supported via NASA grant NAG15-2730. VMK thanks D. Chakrabarty, L. Cominsky, T. Hamilton, P. Harrison, M. van Kerkwijk, and T. Prince for useful discussions. VMK received support for this work through a Princeton University Higgins Instructorship, and from NASA via a Hubble Fellowship through grant number H12-1061.01-94A from the Space Telescope Science Institute, which is operated by the Association of Universities for Research in Astronomy, Inc., under NASA contract NAS5-26555. Some of the research described in this paper was carried out at the Jet Propulsion Laboratory, California Institute of Technology. This research has made use of the Simbad database, operated at CDS, Strasbourg, France.

*preparation of
AJASR*

References

- Arons, J. & Tavani, M., 1993. *ApJ*, 403, 249.
- Bell, J. P., Bailes, M. & Bessell, M. S., 1993. *Nature*, 364, 603.
- Bell, J. P., Bessell, M. S., Stappers, B., Bailes, M. & Kaspi, V. M., 1995. *ApJ*, . submitted.
- Bjorkman, J. E. & Cassinelli, J. P., 1993. *ApJ*, 409, 429.
- Buecheri, R., Bennett, K., Biggiani, G. P., Caraveo, P. A., Bloemen, J. B. G. M., Hermsen, W., Borriakoff, V., Kanbach, G., Manchester, J. L. & Masnou, J. L., 1983. *A&A*, 128, 245.

- Cassinelli, J. D., Cohen, D. H., MacFarlane, J. J., Sanders, W. T. & Welsh, B. Y., 1994. *ApJ*, 421,705.
- Cominsky, L., Roberts, M. & Johnston, S., 1994. *ApJ*, 427,928.
- Cordes, J. M., Romani, R. W. & Lundgren, S. C., 1993. *Nature*, 362,133.
- Córdova, F. A., Hjellming, R. M., Mason, K. O. & Middleditch, J., 1989. *ApJ*, 345,451.
- Ellison, D. C., Jones, F. C. & Reynolds, S. P., 1990. *ApJ*, 360, 702.
- Fritz, G., Henry, R. C., Meekins, J. F., Chubb, T. A. & Friedmann, H., 1969. *Science*, 164, 708.
- Gallant, Y. A. & Arons, J., 1994. *ApJ*, 435,230.
- Gorenstein, P., 1975. *ApJ*, 198,95.
- Greiner, J., Tavani, M. & Belloni, T., 1994. *ApJ*, . preprint.
- Grove, J. E., Tavani, M., Purcell, W. R., Johnson, W. N., Kurfess, J. D., Strickman, M. S. & Arons, J., 1995. *ApJ*, . submitted.
- Halpern, J. & Ruderman, M., 1993. *ApJ*, 415, 286.
- Harding, A., 1995. In: *Millisecond Pulsars: A Decade of Surprise*, eds Fruchter, A., Tavani, M. & Backer, D., *Astronomical Society of the Pacific Conference Series*.
- Hirayama, M., Nagase, F., Tavani, M. & Kaspi, V. M., 1995. *PASJ*, . in preparation.
- Hoshino, M., Arons, J., Gallant, Y. A. & Langdon, A. D., 1992. *ApJ*, **390,454**.
- Johnston, S., Lyne, A. G., Manchester, R. N., Kniffen, D. A., D'Amico, N., Lim, J. & Ashworth, M., 1992a. *MNRAS*, 255,401.
- Johnston, S., Manchester, R. N., Lyne, A. G., Bailes, M., Kaspi, V. M., Qiao, G. & D'Amico, N., 1992b. *ApJ*, 387,1,37.
- Johnston, S., Manchester, R. N., Lyne, A. G., Nicastro, I. & Spyromilio, 1994. *MNRAS*, 268, 430.
- Johnston, S., Manchester, R. N., Lyne, A. G., D'Amico, N., M., B., Gaensler, B. M. & Nicastro, I., 1995. *MNRAS*, . in preparation.
- Kaspi, V. M., Johnston, S., Bell, J. F., Manchester, R. N., Bailes, M., Bessell, M., Lyne, A. G. & D'Amico, N., 1994. *ApJ*, 423, L43.

- Kennel, C. F. & Coroniti, F. V., 1984. *ApJ*, 283, 694.
- King, A. & Cominsky, L., 1994. *ApJ*, 435, 411.
- Kochanek, C. S., 1994. *ApJ*, 406, 638.
- Kulkarni, S. R. & Hester, J. J., 1988. *Nature*, 335, 801.
- Kundt, W. & Krotscheck, E., 1980. *A&A*, 83, 1.
- Lai, D., Bildsten, L. & Kaspi, V. M., 1995. *ApJ*, in preparation.
- Leahy, D. A., Darbro, W., Elsner, R. F., Weisskopf, M. C., Sutherland, P. G., Kahn, S. & Grindlay, J. E., 1983. *ApJ*, 266, 160.
- Lucy, L. B., 1982. *ApJ*, 255, 286.
- MacFarlane, J. J. & Cassinelli, J. P., 1989. *ApJ*, 347, 1090.
- McCollum, B., Castelaz, M. W. & Bruhweiler, F. C., 1995. *ApJ*, in preparation.
- Meurs, E. J. A., Pijpers, A. J. M., Pols, O. R., Waters, L. B. F. M., Coté, J., van Kerkwijk, M. H., van Paradijs, J., Burki, G., Taylor, A. R. & de Martino, D., 1992. *A&A*, 265, L41.
- Nagase, F., 1989. *PASJ*, 41, 1.
- Ögelman, L., 1995. III: Millisecond Pulsars: A Decade of Surprise, eds Fruchter, A., Tavani, M. & Backer, D., *Astronomical Society of the Pacific Conference Series*.
- Pallavicini, R., Golub, L., Rosner, R. & Vaiana, G., 1981. *ApJ*, 248, 279.
- Rees, M. J. & Gunn, J. E., 1974. *MNRAS*, 167, 1.
- Seward, F. D. & Harnden, F. R., 1982. *ApJ*, 256, L45.
- Seward, F. D., Harnden, F. R. & Helfand, D. J., 1984. *ApJ*, 287, L19.
- Shapiro, S. L. & Teukolsky, S. A., 1983. *Black Holes, White Dwarfs and Neutron Stars. The Physics of Compact Objects*, Wiley- Interscience, New York.
- Skinner, G. K., Bedford, D. K., Elsner, R. F., Leahy, D., Weisskopf, M. C. & Grindlay, J., 1982. *Nature*, 297, 568.
- Slettebak, A., 1988. *PASP*, 100, 770.
- Snow, C. P., 1982. *ApJ*, 253, L39.

- Stella, L. & Angelini, L., 1992. XRONOS, NASA-IBM, ASARC.
- Tanaka, Y., Inoue, H. & Holt, S. S., 1994. PASJ, 46, L37.
- Tavani, M. & Arons, J., 1995. ApJ, . in preparation.
- Tavani, M., Arons, J. & Kaspi, V. M., 1994. ApJ, 433, 1,37.
- Tavani, M., 1994. In: The Gamma-Ray Sky with COMPTON GRO and SIGMA, eds Signore, M., Salati, P. & Vedrenne, G., Kluwer Academics. in press.
- Taylor, J. H. & Cordes, J. M., 1993. ApJ, 411, 674.
- vanden Heuvel, E. P. J. & Rappaport, S., 1987. In: Physics of Be Stars, eds Slettebak, A. & Snow, T. P., Cambridge University Press.
- Waters, L. B.F. M., Taylor, A. R., vanden Heuvel, E. P. J., Habels, G. M. H. J. & Persi, P., 1988. A&A, 198, 200.
- Waters, L. H. M., 1986. A&A, 162, 121.
- Westerlund, B. E. & Garnier, R., 1989. Astron. Astrophys. Suppl. Ser., 78, 203.
- White, N. E., Swank, J. H. & Holt, S. S., 1983. ApJ, 270, 711.
-

Astrometric, Spin, and Radio Parameters

Right Ascension, α (J2000)	13 ^h 02 ^m 47 ^s .68(2)
Declination, δ (J2000)	63°50′08″.6(1)
Dispersion Measure, ΔM	46.75(8) pc cm ⁻³
Period, P	47.762053919(4) ms
Period Derivative, \dot{P}	2.2793(4) $\times 10^{-15}$
Period \dot{p} poc	MJD 48053.44
Spin-down Age, τ	3 $\times 10^5$ yr
Magnetic Field, B	3 $\times 10^{11}$ G
Spin-down Luminosity, \dot{E}	8 $\times 10^{35}$ erg s ⁻¹

Orbital Parameters

Orbital Period, P_b	1236.79() days
Projected semi-major axis, $a_p \sin i$	1295.98(1) t s
Longitude of periastron, w	38°.6548(2)
Eccentricity, e	0.869836(2)
Periastron Epoch, T_0	MJD 48124.358 (2)

Table : Spin, astrometric, and orbital parameters for PSR J 259–63 from Johnston *et al.* (1994) The inclination ι the plane σ the orbit i is measured with respect to the plane σ the sky, and ω is measured from the line σ nodes.

Date	MJD	ϕ (10^{12} cm)	s/R_c
Dec. 20, 1993	49349.0	16°	36
Jan. 10, 1994	49362.2	7°	24
Jan. 26, 1994	49378.5	89°	44

Table 2: Summary of PSR 111259--63 system geometry near *ASCA* observations. The true anomaly ϕ is 0° at periastron. The separation between tilt: pulsar and Be star center, s , was deduced assuming $M_c = 1 M_\odot$ and $M_p = 1.4 M_\odot$, and R_c is the Be star radius, assumed to be $6R_\odot$.

MJD	Count Rates (cts S ⁻¹)			
	SIS0	SIS1	GIS2	GIS3
49349.0	0.613	0.499	0.437	0.499
49362.2	0.335	0.271	0.236	0.283
49378.5	0.576	0.433	0.427	0.493

Table 3: Count rates for the four *ASCA* instruments for each observing epoch.

MJD	N_{H} (10^{22} cm^{-2})	Photon 111(ICX)	1-10 keV Flux ($10^{-11} \text{ erg cm}^{-2} \text{ s}^{-1}$)	Fe Emission Line Flux ($10^{-6} \text{ photons cm}^{-2} \text{ s}^{-1}$)
49349.0	0.56(2)	1.71(4)	3.17(14)	" < 7.5
49362.2	0.53(3)	1.86(4)	1.50(7)	< 9.8
49378.5	0.50(3)	1.56(4)	3.04(16)	< 9.7

Table 4: Model parameters for *ASCA S1S* observations of PSR B1259-63 assuming a power law spectrum. Numbers in brackets represent the 90% confidence interval uncertainties in the last digit quoted. The uncertainties quoted are statistical, and do not include any contribution for unknown systematic calibration errors. The last column contains 90% confidence upper limits for flux in a 6.4 keV or 6.7 keV emission line having width 10 eV.

MJD	T' (s)	N_γ	P_{obs} (ms)	\dot{P}_{obs}	P (ms)	\dot{P}
49349.0	44,289	19,282	47.7608264	-4.899×10^{-12}	47.762309	0.000
49362.2	110,447	18,496	47.7514099	-5.739×10^{-12}	47.762311	0.069
49378.5	46,113	15,587	47.7527459	$+2.647 \times 10^{-12}$	47.762314	0.075

Table 5: Summary of characteristics of the *ASCA* data relevant to the pulsation search. The MJD is the at the start of the observation, T' is the duration of the observation (longer than the exposure time because of earth occultations, South Atlantic Anomaly passages, etc.), N_γ is the total number of GIS photons, P_{obs} is the barycentric period at the start of the integration, \dot{P}_{obs} is the effective period derivative due to the pulsar’s acceleration in its orbit, P is the period as observed in a reference frame at rest with respect to the pulsar, and \dot{P} is the 90% confidence upper limit on the pulsed fraction obtained via epoch-folding and assuming a sine-wave profile (see §3.2). The spin parameters were obtained using the Johnston *et al.* 1994) ephemeris.

MJD	P Range (ms)	\dot{P} Range ($\times 10^{-12}$)
49349.0	47.7600 - 47.7616	-20.0 - 0.0
49362.2	47.7510 - 47.7520	-7.0 - -4.0
49378.5	47.7520 - 47.7535	0.0 - 18.0

Table 6: Summary of P - \dot{P} pulsation search. The tabulated P range was searched in steps of $P^2/5T'$, and the \dot{P} range in steps of $P^2/5T'^2$.

FIGURE CAPTIONS

Fig. 1.- Schematic representation of the PSR B1259-63 binary orbit with the locations of the pulsar during all published X-ray detections indicated. CRJ94 is Cominsky, Roberts & Johnston (1994), GTB95 is Greiner, Tavani & Belloni (1994), and the observations labeled ASCA are the subject of this paper. The cross indicates the location of the center of mass of the system.

Fig. 2.- PSR B1259-63 velocity curve and the *ASCA* observing epochs. The upper panel is the pulsar's velocity curve as determined from radio timing data (Johnston *et al.* 1992b). The region between the vertical lines is expanded in the lower panel, in which the epochs of the *ASCA* observations described here are high-lighted.

Fig. 3- Image of the GIS2 field of view for the MJD 49378 observation. Those for the first two observations are similar. A logarithmic scale was used for this image, and pixels are $1'$. North is up and west is to the right. The brighter source is PSR 11259-63 while the weaker source is a serendipitously discovered source unassociated with the PSR B1259-63 system. The weak enhancement seen in 011 east side of the image is due to the imperfectly removed *ASCA* calibration source. (TOBE REVISED)

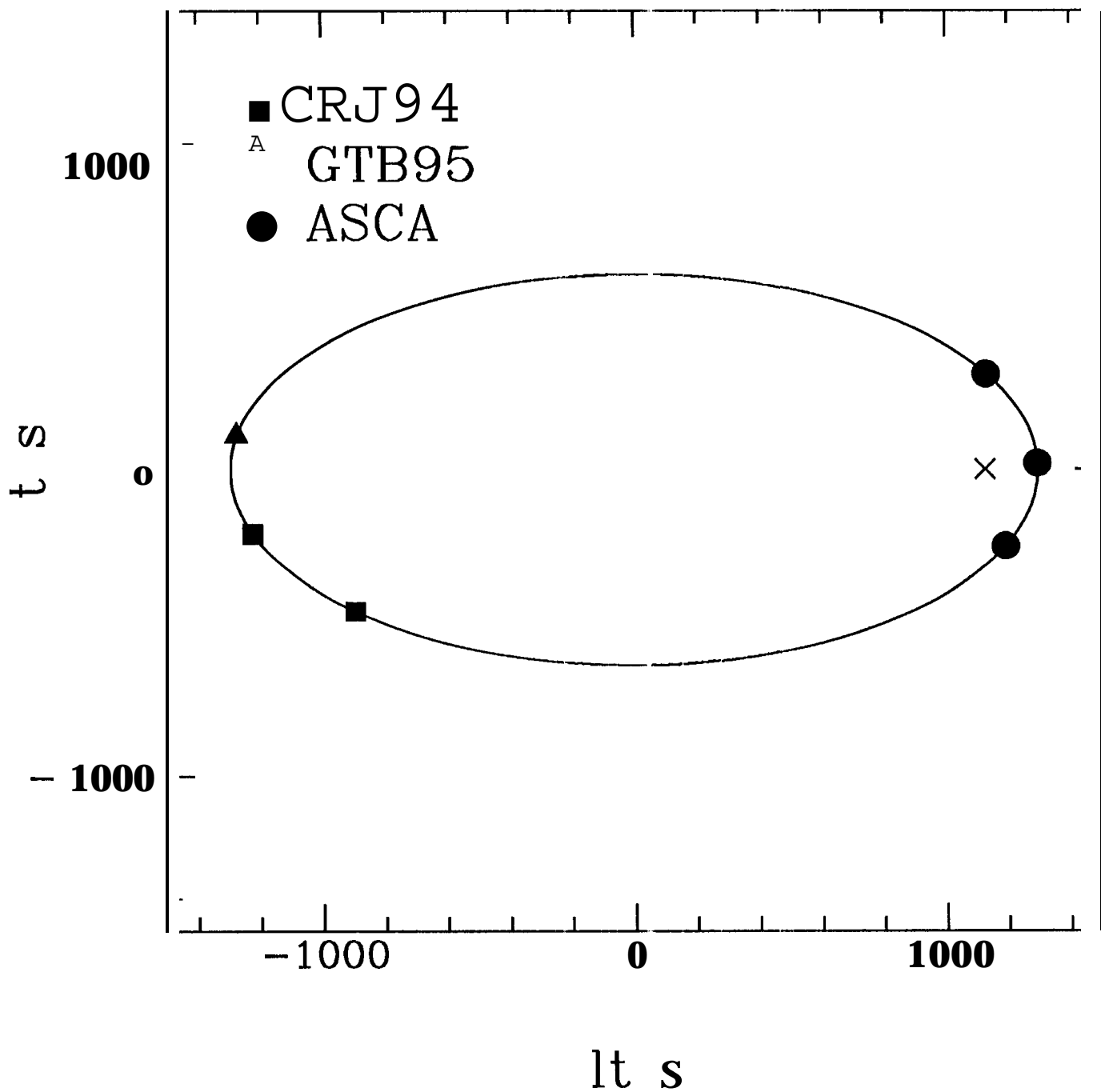
Fig. 4.- Image of the **S1S0** field of view for the MJD 49378 observation. Those for the first two observations are similar. The signature “cross-pattern,” typical for a point source, is apparent.

Fig. 5.- GIS2 light curves for PSR B1259--63 at the three observing epochs. The data shown here have been binned in 240 s intervals. Light curves for the other instruments are similar.

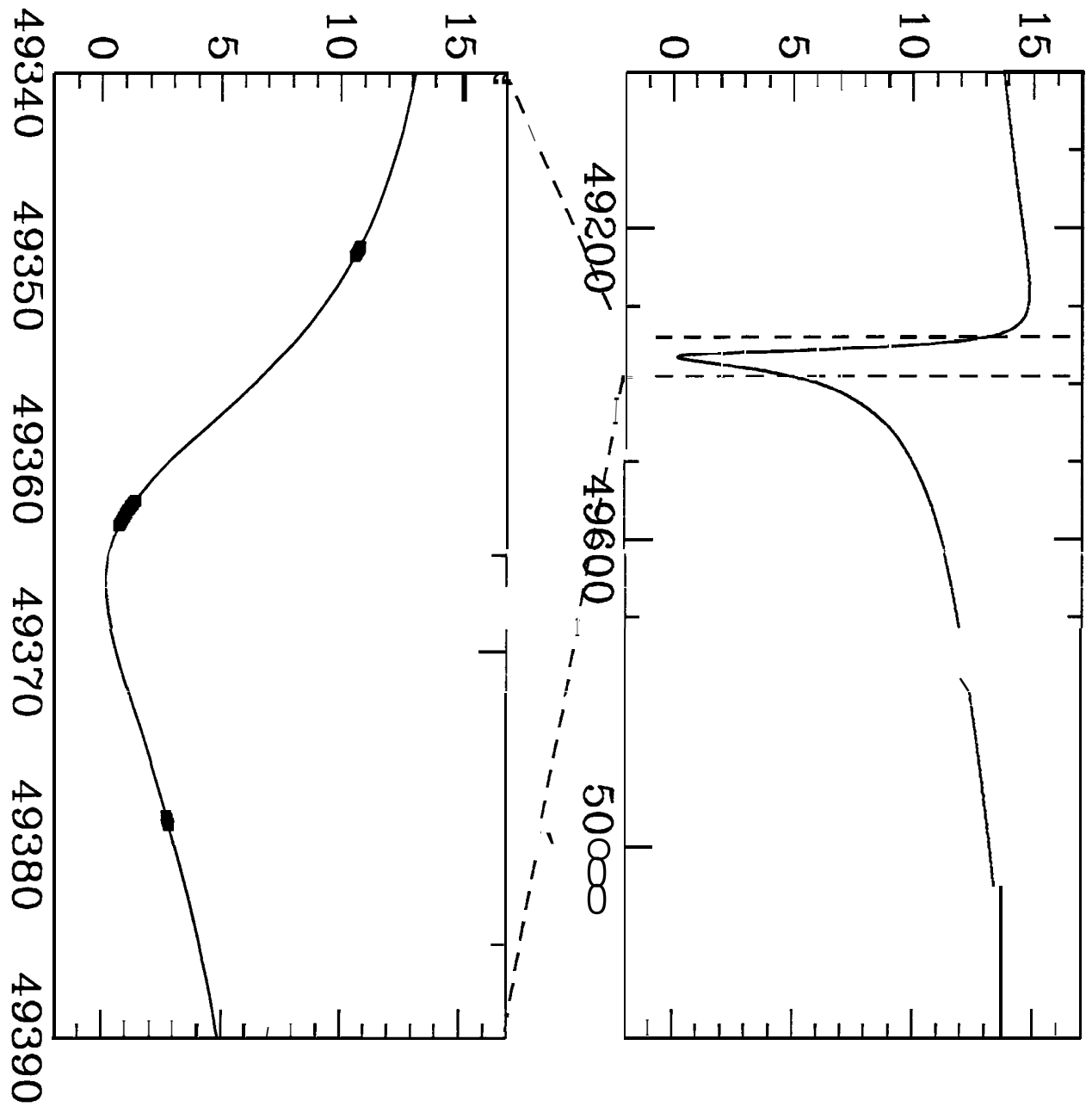
Fig. 6.- ASCA SIS spectra at the three observing epochs.

Fig. 7.- Contour plots of the confidence levels for the fit values of N_{H} and photon index at the three observing epochs. The contours are the 68%, 90% and 99% confidence levels, and were obtained while holding the 1-10 keV flux fixed at the values given in Table 4.

Fig. 8.- The parameter S , defined in Eq. 2, versus trial period for MJD 49349 combined GIS2 and GIS3 data corrected for a variable Doppler shift using Eq. 1. The features in the plot are not statistically significant.

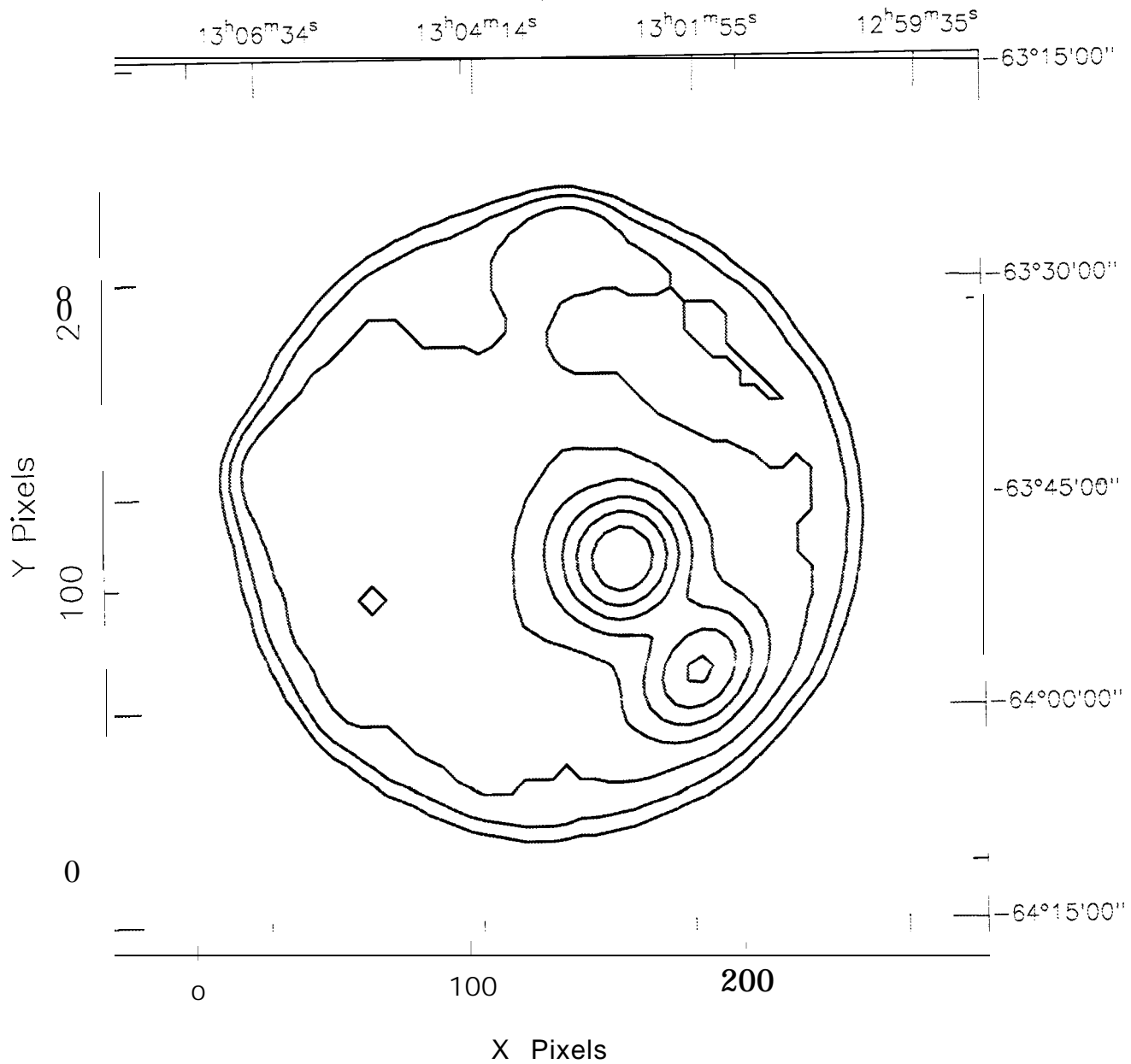


Period (μs , offset from $47'750 \mu\text{s}$)



Modified Julian Date

ASCA GIS IMAGE
PSR1259-63 / MJD 49362



ASCA SIS IMAGE
PSR1259-63 / MJD 49362

13^h03^m29^s 13^h02^m58^s 13^h02^m28^s 13^h0^m57^s

